

They best work when handling single-phase liquid flow. In fact, the presence of gas phase in liquid flow causes head loss and low efficiency, therefore performance deterioration and higher operational costs. The degradation reflects both a heterogeneity of the liquid/gas mixture and a change of flow structure within the pump under the sliding effect between the phases, but the physical mechanism that governs these phenomena is neither well understood nor controlled.

The inlet gas volume fraction (*IGVF*) is found to play a major role in defining the centrifugal pumps behavior. Increasing *IGVF* causes a growing degradation of performance, a changing of two-phase flow patterns inside the impeller, and for a critical value it causes the so-called "Gas locking" where there is an obstruction by gas of the impeller passages and head goes to zero. According to [Gülich \(2010\)](#), there are no universal critical values of *IGVF* and seem to be specific for each pump based on its geometric features, fluids properties and operating conditions.

Axial and mixed type pumps better handle two-phase flows. The outcome is the necessary stages to raise sufficient head for operation, resulting in bulky equipment.

The two-phase flow pumping was mainly studied by nuclear, chemical and petroleum experts and researchers, because they have to cope with related industry problems. Theoretical and numerical, but mostly experimental researches have been done to analyze the behavior of the centrifugal pumps in two-phase flows, but still further investigations are needed.

The following is a review of selected literature on centrifugal pump two-phase flows that inspired the present study and helped to comprehend the results.

[Murakami et al. \(1974\)](#) introduced "Effects of entrained air on the performance of a centrifugal pump". [Chen et al. \(1980\)](#) investigated numerically and experimentally two-phase flows of centrifugal pumps. In particular, he noted that pumps suffer performance degradation when increasing the volume fraction of gas.

[Minemura et al. \(1980; 1998\)](#) carried out an outstanding experimental and theoretical work with regard to the movement of air bubbles in a centrifugal pump impeller. The authors demonstrated that the main forces that govern the bubble motion within centrifugal impellers are those corresponding to drag and pressure gradient around the bubble. Besides, the bubbles tend to deviate from the streamlines of liquid. This tendency enhances as the bubble diameter increases. The resultant of the forces tends to slow the bubble and to move them to the pressure side of the impeller blade where they accumulate, consequently causing phase separation.

[Furuya \(1985\)](#) found that the head degradation in two-phase flows is mainly caused by higher acceleration on liquid phase and deceleration on gas phase than in the case of single-phase flows. He

developed an analytical model for prediction of two-phase flow pump performance based on one dimensional control volume method.

[Chan et al. \(1999\)](#), made numerous experiments on nuclear reactor pumps. The results were used by [Noghrehkar et al. \(1995\)](#) to develop and validate an analytical model for two-phase pumps. The physical mechanisms responsible for head degradation were also investigated. One of possible causes is that when the void fraction exceeds a certain point, the flow in the inter-blade pump passages stratifies under the important transverse pressure gradient.

[Kosyna et al. \(2001\)](#), made an experimental investigation of unsteady pressure distribution over an impeller blade in two-phase flow conditions. He concluded that the loss of the pump head with increasing gas volume fraction is a result of the drop of the blade pressure rise due to the de-mixing of the two phases.

[Caridad et al. \(2008\)](#) made numerical studies to characterize a centrifugal pump behavior under two-phase flow conditions by considering the effect of bubble size and gas volume fraction. They detect that the physical phenomena responsible for the head fall is linked to a gas pocket accumulating on the pressure side of the blade associated with a change of the flow angle at the impeller outlet, which diminish the capacity of the impeller to change the kinetics momentum of the mixture.

[Gamboa et al. \(2010\)](#) conducted a series of experimental tests to study the gas pocket behavior in a centrifugal pump at different operating conditions and fluid properties. They noticed that the gas pocket is formed as a consequence of bubble coalescence within impeller passage. The critical gas fraction varies as a function of gas density, rotational speed and intake pressure, while its stability is a function of surface tension and bubble size.

[Müller et al. \(2015\)](#) performed numerical studies to predict the flow of liquid-gas mixture in radial pumps. Head as well as blade pressure profiles were compared to experimental data.

[Schäfer et al. \(2017\)](#) led experimental studies on the effects on hydraulic power of gas entrainment in centrifugal pumps designed for conveying liquids only. It has been found that increasing gas entraining in two-phase flow regime leads to a higher and discontinuous performance drop. Moreover, gamma-ray tomography has been applied to quantify local phase fraction distributions inside the rotating impeller. Various internally accumulated gas patterns have been identified and associated with characteristic pump performance behaviors.

[Monte Verde et al. \(2017\)](#) conducted high-speed imaging techniques aiming at determining gas-liquid flow patterns inside a centrifugal pump impeller. It was observed that the intensity of pump performance degradation is directly influenced by the flow pattern within the impeller. Maps correlating flow pattern and pump performance

were set for different operating conditions.

Shao *et al.* (2018) investigated flow patterns of the gas-liquid mixture in a centrifugal pump by using high-speed photography, and the performance of the pump was measured under different conditions. It was observed that the flow patterns in the impeller and volute can be classified into four categories with increasing inlet gas volume fraction, with a decrease of the differential pressure of the pump, and once it reaches the critical value, some bubbles in the volute begin to flow back into the impeller near the volute tongue.

Numerical studies of two-phase flows in centrifugal pumps are still sought in the literature for thorough flow analysis. The aim of the present study is to provide a new highlight on performance evolution of a centrifugal pump when handling two-phase flows by comparing with single-phase behavior in order to identify the physical mechanism responsible for the head fall down.

CFD calculations are carried out at design flow rate with varying inlet gas volume fraction. Volute interaction effects are also investigated. From analysis conclusion, concepts are suggested to improve performance in order to construct efficient centrifugal pumps specially designed for handling two-phase flows.

2. GOVERNING EQUATIONS

2.1 Assumptions

The Eulerian approach is used for obtaining phase distributions and their influence on pressure and velocity fields. The flow is regarded as non-homogeneous, that is a two-fluid model, which allows a separate velocity field for each phase with a shared common pressure field.

The liquid is assumed the continuous phase and the gas is supposed to stay in bubbly dispersed mode and entrained by liquid.

Governing equations are set for each phase. Turbulence models are also used for each phase.

2.2 Formulation

The unknowns of the problem are the velocity vectors of gas and liquid U_g and U_l , the pressure of gas and liquid p_g and p_l , and the volume fraction of gas α .

ρ_g and ρ_l are respectively density of gas and liquid.

τ is the shear stress tensor. t is time and x the spatial dimensions. Gravity is neglected.

The governing equations for two-phase flow are:

Mass conservation equation for gas:

$$\frac{\partial(\alpha\rho_g)}{\partial t} + \frac{\partial(\alpha\rho_g U_{gi})}{\partial x_i} = 0 \quad (1)$$

Mass conservation equation for liquid:

$$\frac{\partial((1-\alpha)\rho_l)}{\partial t} + \frac{\partial((1-\alpha)\rho_l U_{li})}{\partial x_i} = 0 \quad (2)$$

The gas volume fraction is defined by:

$$\alpha = \frac{Q_g}{(Q_g + Q_l)} \quad (3)$$

Momentum equation for gas:

$$\frac{\partial(\rho_g U_{gi})}{\partial t} + \frac{\partial(\alpha\rho_g U_{gj} U_{gi})}{\partial x_j} = -\frac{\partial p_g}{\partial x_i} + \frac{\partial \tau_{gij}}{\partial x_j} \quad (4)$$

Momentum equation for liquid:

$$\frac{\partial(\rho_l U_{li})}{\partial t} + \frac{\partial((1-\alpha)\rho_l U_{lj} U_{li})}{\partial x_j} = -\frac{\partial p_l}{\partial x_i} + \frac{\partial \tau_{lij}}{\partial x_j} \quad (5)$$

Equation resulting from the hypothesis of a shared pressure field (adopted in two-phase flow models):

$$p_g = p_l \quad (6)$$

2.3 Drag Force

The total drag force F_D acting on spherical bubbles per unit volume can be written as follows:

$$F_{DI} = -F_{Dg} = \frac{3}{4} C_D \frac{\rho_l}{d} \alpha |U_g - U_l| (U_g - U_l) \quad (7)$$

The dimensionless drag coefficient C_D is calculated by the Schiller-Naumann drag law (Müller *et al.*, 2015):

$$\begin{cases} C_D = \frac{24}{Re} (1 + 0.15 Re^{0.687}) & \text{for } Re \leq 1000 \\ C_D = 0.44 & \text{for } Re > 1000 \end{cases} \quad (8)$$

Where Re is the Reynolds number based on bubble diameter d , the slip velocity between the phases ($U_g - U_l$), the density ρ_l and the dynamic viscosity μ_l of the liquid:

$$Re = \frac{\rho_l d |U_g - U_l|}{\mu_l} \quad (9)$$

Both phases are considered incompressible. According to Müller *et al.* (2015), treatment of the gas phase as incompressible enhances significantly the stability of the solver and hardly changes the results.

2.4 Turbulence Models

Continuous Phase (liquid): *SST* (Shear Stress Transport) *K- ω* eddy viscosity two-equation turbulence model.

Dispersed phase (gas): algebraic eddy viscosity zero-equation turbulence model.

3. NUMERICAL PROCEDURE

3.1 Geometry and Flow Parameters

A centrifugal pump usually operating in water and

not specially designed to operate in two-phase flows is chosen to characterize its behavior. The selection is based upon its known geometry and flow parameters.

The pump is modeled as a set of complete 360° geometries of the impeller and the volute in order to analyze whole flow fields and to capture the full interaction effects. An entry duct is added to apply proper inlet boundary conditions. Table 1 summarizes the main features in industry units of the components and operating conditions of the selected pump. The blade angles are counted from tangential direction.

Table 1 Geometry and flow specifications

Flow conditions		
<i>Speed of rotation</i>	N	1470 rpm
<i>Specific speed</i>	N_s	32
<i>Design flow rate</i>	Q_0	590 m ³ /h
<i>Design head</i>	H_0	49 m
Impeller		
<i>Number of blades</i>		5
<i>Blade thickness</i>		8 mm
<i>Inlet radius</i>		75 mm
<i>Inlet width</i>		85.9 mm
<i>Inlet blade angle</i>		20°
<i>Outlet radius</i>		204.2 mm
<i>Outlet width</i>		42 mm
<i>Outlet blade angle</i>		27°
Volute		
<i>Cutwater radius</i>		218 mm
<i>Inlet width</i>		50 mm
<i>Outlet radius</i>		100 mm

3.2 Mesh Structure

The pump is completely meshed with unstructured tetras (see Fig. 1). Tetras are more flexible elements to model complex passage geometries but the outcome is a larger problem dimension. Mesh refinements are placed at particular locations like inlet/outlet, blade edges, component interfaces and walls. Special care is made at walls to apply proper automatic near-wall treatment. A preliminary study for mesh sensitivity has led to a total number of nodes around 1.2 million.

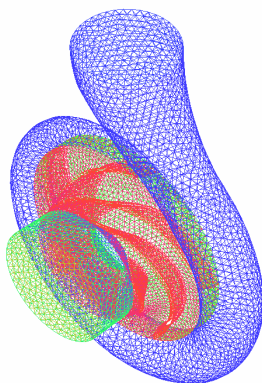


Fig. 1. Pump mesh.

3.3 Computations

Non-miscible air/water mixture is used to characterize two-phase flows through the pump. Bubbles are of size 0.5 mm in mean diameter. Flows undergo an isothermal process. The simulations are carried out at design flow rate with varying inlet gas volume fraction IGVF from 0% (single-phase mode) to 20% (two-phase mode). Boundary conditions are total pressure inlet / mass flow rate outlet. Walls are considered adiabatic and non-slip. Computations are achieved using licensed ANSYS CFX code. Three-dimensional, steady Reynolds averaged Navier-Stokes equations are solved. Turbulence is modeled for each phase, in combination with automatic near-wall treatment. Frozen rotor calculations are performed at a prescribed impeller position for quick and sufficiently accurate performance evaluation (Müller *et al.*, 2015). The general convergence criteria is set to momentum residues below 10⁻⁴.

4. RESULTS AND DISCUSSION

4.1 Head Rise

Head is an important parameter to measure pump performance. It is calculated by outlet to inlet total pressure difference.

For two-phase flows, the delivered head H is estimated by the following formulae (Shao *et al.*, 2018):

$$H = (1 - \chi) \left[\frac{(p_2 - p_1)}{\rho G} + \frac{(U_2^2 - U_1^2)}{2G} \right]_l + \chi \left[\frac{(p_2 - p_1)}{\rho G} + \frac{(U_2^2 - U_1^2)}{2G} \right]_g \quad (10)$$

Subscripts l and g indicate mean values at respectively inlet and outlet of the pump. G is the acceleration of gravity.

χ is the quality of the mixture in mass defined as:

$$\chi = \left[\frac{\alpha \rho_g}{\alpha \rho_g + (1 - \alpha) \rho_l} \right] \quad (11)$$

The two-phase normalized head star H^* is defined as the ratio of the delivered head H to the design single-phase head H_0 :

$$H^* = \left[\frac{H}{H_0} \right] \quad (12)$$

Figure 2 illustrates the head characteristic curve when varying inlet gas volume fraction IGVF from 0% (single-phase mode) to 20% (two-phase modes). The first run in single-phase mode gives results in good agreement with manufacturer's data. For two-phase flow modes, the case of 1% IGVF reveals a head almost equal to single-phase situation. The gas flow stays at dispersed mode everywhere and no influence on pump single-phase performance has

been detected (Shao *et al.*, 2018).

After 1% *IGVF*, the characteristic curve shows a continuous, steep and linear-shaped drop of head with increasing inlet gas volume fraction, reaching significant amounts (only 46% of original head for 20% *IGVF*). It demonstrates that centrifugal pumps are sensitive to the presence of gas in liquid flows and leads to a deterioration of performance even at design flow conditions. This is a general behavior for centrifugal pumps handling two-phase flows, also reported by several other authors but with diverse tendencies and *IGVF* ranges (Kosyna *et al.*, 2001; Caridad *et al.*, 2008; Gamboa *et al.*, 2010; Schäfer *et al.*, 2017; Shao *et al.*, 2018).

It may be worthwhile to mention that the head should break down to zero soon after 20% *IGVF*, once exceeding a critical value because of gas locking occurrence. The critical behavior of the pump handling two-phase flows was not investigated in the present study.

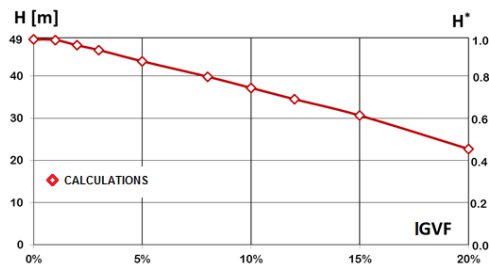


Fig. 2. Head rise and Head star vs IGVF for $Q_0=590 \text{ m}^3/\text{h}$ and $N= 1470 \text{ rpm}$.

4.2 Velocity Fields

Centrifugal pumps have poor capability for handling two-phase flows. The causes for head loss, and therefore performance deterioration, can be explained by analyzing flow field variations inside the impeller between single-phase and two-phase situations.

Relative velocity distributions for water and air are extracted from computations to show the flow structure within the impeller. Blade-to-blade velocity fields are illustrated at three selected constant-span surfaces from hub to shroud, as indicated in Table 2.

Table 2 Span specifications

Ratio to total span	0.2	0.5	0.8
Location	Near the hub	Mid-span	Close to shroud

Single-phase mode: Figure 3 illustrates the velocity fields for water in single-phase mode. The analysis of the flow fields reveals the classical flow structure inside a backswep centrifugal impeller. It should well be noted that the meridional curvature exerts a crucial influence on the span-wise velocity distribution, while the blade forces and rotation determine the blade-to-blade distribution. In summary, the balance of forces leads to an increase

of relative velocity from pressure side to suction side in the blade-to-blade section and from hub to shroud in the meridional section. The figure shows a low velocity region confining at the pressure side of the blades, much more pronounced near the hub than close to shroud. Higher velocity dominates at the suction side of the blades. The observed flow pattern is a result of blade forces acting on the fluid. An impeller transfers energy to the fluid when a lower pressure prevails on the suction side of a blade than on the pressure side (Kosyna *et al.*, 2001). Therefore, the flow around a blade tends to produce a maximum velocity near the suction side, and consequently, a deficit in the pressure side. This flow configuration is the so-called "jet/wake" structure described in classic turbomachinery books (Gülich, 2010). The trend is altered near the exit part of the impeller, where there is less guidance by the blades; secondary flows brought by Coriolis forces partly or completely equalize this velocity difference (Gülich, 2010).

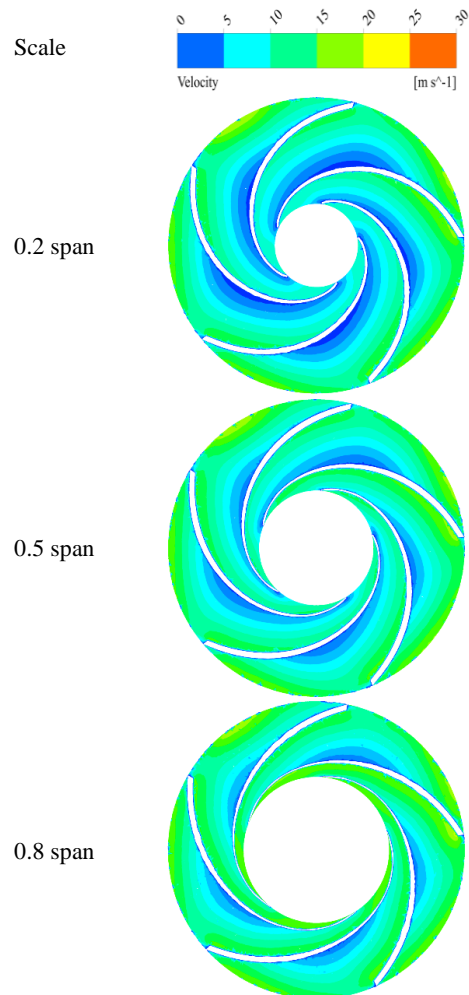


Fig. 3. Impeller velocity distribution for single-phase mode.

Two-phase mode: For illustrative purpose, only the 10% *IGVF* case is used to characterize the two-phase pump behavior. Figures 4 and 5 illustrate respectively the velocity fields for water and air in

two-phase mode. The analysis of the flow fields for both water and air reveals similar flow structure as for single-phase case; a low velocity confining near the pressure side of the blades and higher velocity close to suction side, with a strong variation from hub to shroud. However, the velocity fields show that a slip exists between phases; water velocity is slightly higher than air velocity. Gas bubbles are entrained by liquid particles and drag forces are acting on them in a stream-wise way.

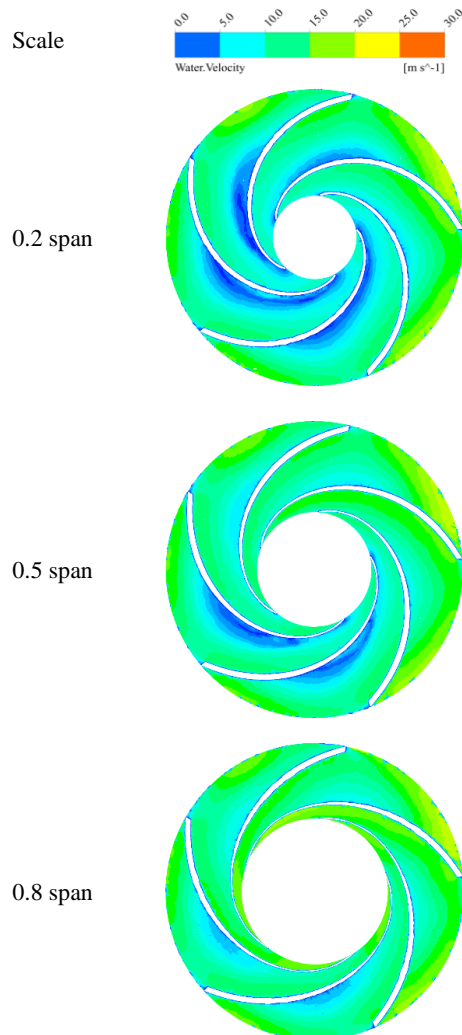


Fig. 4. Impeller water velocity distribution for two-phase mode (IGVF= 10%).

4.3 Phase Distributions

Because of density difference, body forces and inertia dominate the behavior of liquid, while the pressure field and drag primarily determine the distribution of gas. Gas bubbles travel against a strong centrifugal pressure gradient towards the outlet. Gas then tends to accumulate in locations with high deceleration and low velocities. As well as found by Minemura *et al.* (1998), the resultant of forces on a bubble tends to move it towards the pressure side of the blade where they accumulate, consequently causing phase separation (see Fig. 6 from Caridad *et al.*, 2008).

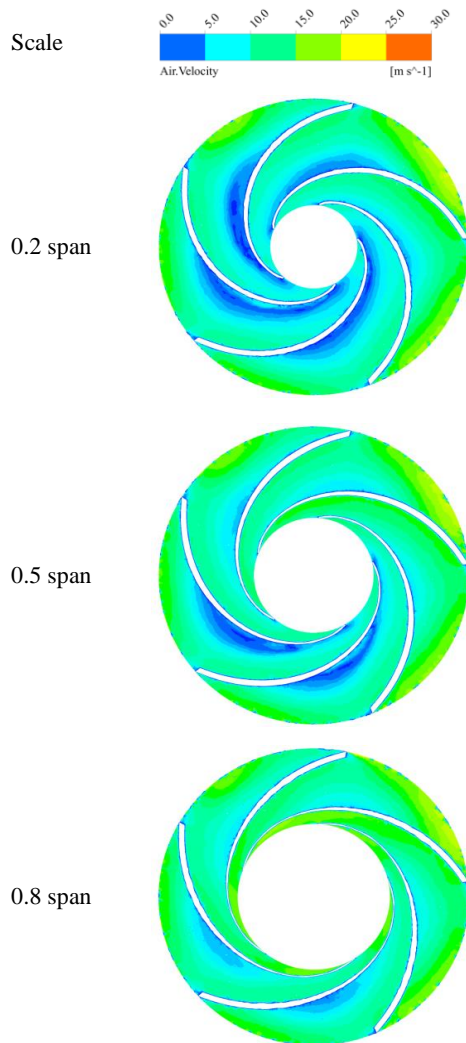


Fig. 5. Impeller air velocity distribution for two-phase mode (IGVF= 10%).

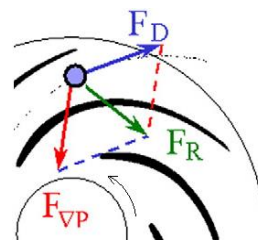


Fig. 6. Forces applied on a bubble.

Figure 7 illustrates the consequence of these factors. The distribution of air volume fraction shows clearly a phase separation between liquid and gas inside the impeller. The gas phase is directed towards the pressure side of the blades where they accumulate. They form what is called a “Gas pocket”, also reported by other authors (Minemura *et al.*, 1998; Caridad *et al.*, 2008). The gas pocket is closely related to stagnation zones inside the impeller: the low flow velocity promotes phase separation and gas accumulation. The gas pocket is more spread near the hub to mid-span, in the inner part of the impeller. It almost disappears close to shroud.

This gas accumulation is a direct cause of performance deterioration: when the gas pocket covers a sufficient portion of the blade length, the head developed by the pump drops sharply. The part of a blade that is covered by a gas pocket transfers little energy (Kosyna *et al.*, 2001). Gas accumulations also block part of the cross section of the impeller passages, resulting in an acceleration of the liquid phase and modification of its streamlines. This flow deviation from single-phase case tends to lower the outlet relative flow angle. The flow is accelerated but the energy transferred does not contribute to increase the static pressure (Caridad *et al.*, 2008).

These mechanisms may be responsible for a main part of that the performance of centrifugal pumps deteriorates. In addition, other factors can contribute; there is an exchange of momentum between gas and liquid phases, generating additional losses which are absent in single-phase flow.

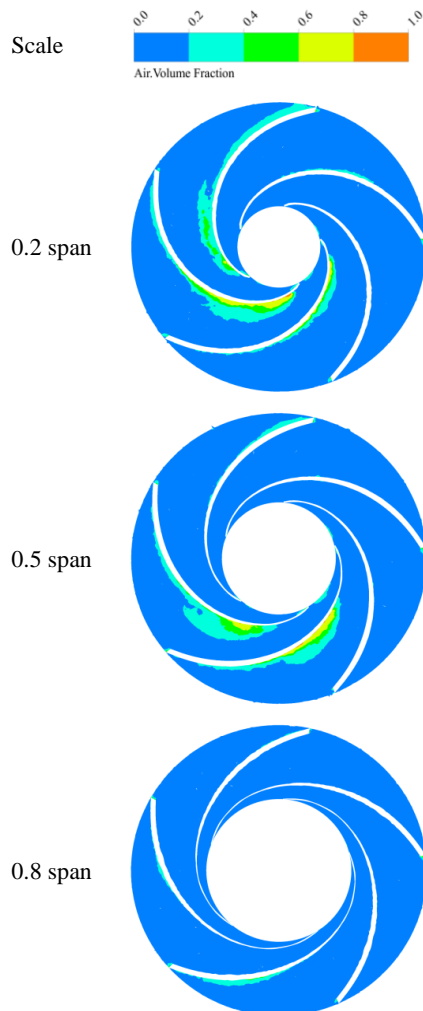


Fig. 7. Impeller distribution of air volume fraction (IGVF= 10%).

4.4 Effects of Interaction with Volute

Regarding the influence of volute interaction on the

flow within the impeller, it can be seen from Figs. 3, 4 and 5 a departure of tendency between single-phase and two-phase flow situations. Figure 8 illustrates the layout of volute with respect to impeller.

In single-phase mode as seen in Fig. 3, flow fields from one impeller passage to another show little variation. The flow structure leaving the impeller is in good arrangement with volute geometry at this design flow rate and the effects of interaction are minor.

The trend is changed in two-phase mode. From Figs. 4 and 5, flow fields from one impeller passage to another and from hub to shroud show strong variations. This reveals that the flow structure leaving the impeller, affected by the presence of gas, is deeply transformed and is no longer in good arrangement with volute geometry even at this design flow rate. The formed gas pocket is found responsible for this flow alteration and consequently is generating flow distortion at the impeller outlet. The presence of gas in liquid flow results in strong interaction effects with volute. This mis-arrangement of the flow with the volute geometry causes disturbances and added losses compared to single-phase situation, which makes head drops.

From Figs. 4 and 5, a noticeable effect of the interaction is the constriction of the low velocity region in blade passages close to volute throat (see Fig. 8). The gas pockets disappeared in these blade passages due to higher flow velocities (see Fig. 7), therefore reducing their nuisance effects.

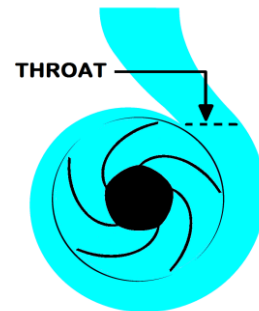


Fig. 8. Volute layout.

4.5 Concepts for Enhancing Two-Phase Pumping

The gas/liquid handling of centrifugal pumps is poor unless special design features are implemented for improving that capacity.

One concept is to make exaggerated "gaps" along hub or shroud between pressure side and suction side of blades, especially at the inner part of the impeller, like that found in semi-open or open impellers, so that leaking flows between these two sides can break-up and detach the gas pocket responsible for head degradation (see Fig. 9).

The next concept is to make "bleeding" holes in the hub or shroud plates that inject liquid from back or

outlet pressure towards incoming flow to homogenize and prevent phase separation. Schäfer *et al.* (2017) described the positive impact of a balancing hole that reduces the accumulation of gas inside the impeller.

Another concept is to exploit the beneficial effect of interaction with volute, by adding throat zones using split-type volute (see Fig. 10).

Owing to these geometric adjustments needed for the suggested concepts, some extra losses are brought to the flow, but surely it can improve two-phase flow handling of centrifugal pumps and reduce performance deterioration. The implementation of these concepts and their effects are under investigation by both experimental and numerical means.

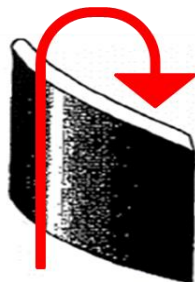


Fig. 9. Flow through gaps between blade sides.

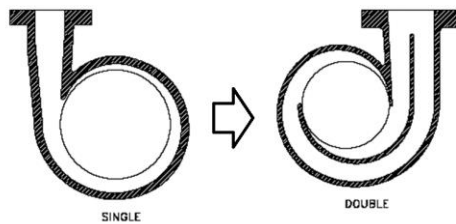


Fig. 10. Split-type volute.

5. CONCLUSION

Numerical simulations of two-phase flows through a centrifugal pump have been performed and presented. The results show that the presence of gas phase in liquid flow causes a significant drop in head rise through the pump comparing to single-phase situation. Phase separation and accumulation of gas on the pressure side of the blades is linked to this performance deterioration. The formed gas pocket results in an obstruction of the passages for liquid flow, reducing energy transfer by the blades and altering the flow structure leaving the impeller. The interaction with volute is stronger in case of two-phase flows even at design conditions. Concepts consisting of geometric adjustments of the pump are suggested to improve two-phase flow handling by centrifugal pumps. Future extension of the study is to investigate further effects from varying flow rate, rotation speed, intake pressure and bubble diameter, as well as from implementing improvement concepts.

REFERENCES

- Caridad, J., M. Asuaje, F. Kenyery, A. Tremante and O. Aguillón (2008). Characterization of a centrifugal pump impeller under two-phase flow conditions. *Journal of Petroleum Science and Engineering* 63, 18-22.
- Chan, A., M. Kawaji, H. Nakamura and Y. Kukita (1999). Experimental study of two-phase pump performance using a full size nuclear reactor pump. *Nuclear Engineering and Design* 193, 159-172.
- Chen, T.H. and W.P. Quapp (1980). Centrifugal pump performance under simulated two-phase flow conditions. In *Proceeding of the ASME*, San Francisco, USA.
- Furuya, O. (1985). An analytical model for prediction of two-phase (non-condensable) flow pump performance. *ASME Journal of Fluids Engineering* 107, 139-147.
- Gamboa, J. and M. Prado (2010). Experimental investigations on a common centrifugal pump operating under gas entrainment conditions. In *Proceeding of the 26th International Pump Users Symposium*, Houston, USA.
- Gülich, J.F. (2010). *Centrifugal Pumps*, second edition. Springer-Verlag, Berlin, Germany.
- Kosyna, G., P. Suryawijaya and J. Friedrichs (2001). Improved understanding of two-phase flow phenomena based on unsteady blade pressure measurements. *Journal of Computational and Applied Mechanics* 2 (1), 45-52.
- Minemura, K. and M. Murakami (1980). A theoretical study on air bubble motion in a centrifugal pump impeller. *Journal of Fluids Engineering* 102, 446-455.
- Minemura, K., T. Uchiyama, S. Shoda and K. Egashira (1998). Prediction of Air-Water Two-Phase Flow Performance of a Centrifugal Pump Based on One Dimensional Two-Fluid Model. *ASME Journal of Fluids Engineering* 120, 327-334.
- Monte Verde, W., J. L. Biazussi, N.A. Sassim and A.C. Bannwart (2017). Experimental study of gas-liquid two-phase flow patterns within centrifugal pumps impellers. *Experimental Thermal and Fluid Science* 85, 37-51.
- Müller, T., P. Limbach and R. Skoda (2015). Numerical 3D RANS simulation of gas-liquid flow in a centrifugal pump with an Euler-Euler two-phase model and a dispersed phase distribution. In *Proceeding of the 11th European Conference on Turbomachinery, Fluid Dynamics and Thermodynamics*, Madrid, Spain.
- Murakami, M. and K. Minemura (1974). Effects of entrained air on the performance of a centrifugal pump. In *Bulletin of the JSME* 17 (110), 1047-1055.

- Noghrehkar, G., M. Kawaji, A. Chan, H. Nakamura and Y. Kukita (1995). Investigation of centrifugal pump performance under two-phase flow conditions. *ASME Journal of Fluids Engineering* 117, 129-137.
- Schäfer, T., M. Neumann, A. Bieberle and U. Hampel (2017). Experimental investigations on a common centrifugal pump operating under gas entrainment conditions. *Nuclear Engineering and Design* 316, 1-8.
- Shao, C., C. Li and J. Zhou (2018). Experimental investigation of flow patterns and external performance of a centrifugal pump that transports gas-liquid two-phase mixtures. *International Journal of Heat and Fluid Flow* 71, 460-469.